

INEEL/CON-05-02597
PREPRINT

Osteoblast Adhesion Of Breast Cancer Cells With Scanning Acoustic Microscopy

C. Miyasaka
R. R. Mercer
A. M. Mastro

March 20 – 23, 2005

28th International Acoustical Imaging
Symposium

This is a preprint of a paper intended for publication in a journal or proceedings. Since changes may be made before publication, this preprint should not be cited or reproduced without permission of the author.

This document was prepared as an account of work sponsored by an agency of the United States Government. Neither the United States Government nor any agency thereof, or any of their employees, makes any warranty, expressed or implied, or assumes any legal liability or responsibility for any third party's use, or the results of such use, of any information, apparatus, product or process disclosed in this report, or represents that its use by such third party would not infringe privately owned rights. The views expressed in this paper are not necessarily those of the U.S. Government or the sponsoring agency.

OSTEOBLAST ADHESION OF BREAST CANCER CELLS WITH SCANNING ACOUSTIC MICROSCOPY

C. MIYASAKA^{*1}

*Department of Physics, Idaho National Engineering and Environmental Laboratory
Idaho Falls, ID 83415, USA*

R. R. MERCER and A. M. MASTRO^{*2}

*Department of Biochemistry and Molecular Biology, The Pennsylvania State University
431S Frear, University Park, PA 16802, USA*

1. Introduction

Once breast cancer has progressed to an advanced stage, it is likely to metastasize to bone, and is usually fatal. However, the process by which breast cancer affects bone tissue is poorly understood [1]. When breast cancer metastasizes to bone, the osteoclasts are constitutively activated, resulting in osteolytic lesions [2]. Kureja *et al* examined nude mice with bone metastasis, and found a significant decrease in bone formation [3]. Similar results have also been reported elsewhere [4]-[5]. Therefore, these observations suggest that breast cancer cells affect osteoblasts in addition to osteoclasts.

When MC3T3-E1 osteoblasts were cultured in cancer cell condition medium, they took on a fibroblast-like morphology and exhibited adhesion characteristics different from those observed in normal medium. The osteoblasts were fixed and stained for actin visualization and for observation of the focal adhesion plaques with optical microscopy. However, since fixation kills the cells, some characteristics of the adhesion may be missed. On the other hand, an acoustic image is formed by reflected ultrasonic waves that are based on the elastic properties of the living cells. Therefore, fixing and staining are not required for mechanical scanning acoustic reflection microscopy [6] (hereinafter called simply "SAM"). Hence, living cells can be easily observed. Further, SAM allows observation not only of the surface but also of the internal structure of the specimen with sub-micrometer resolution [7]-[12]. This report presents the visualization of adhesive conditions of living osteoblasts grown on the substrate using SAM. The results are compared with those obtained with laser scanning confocal microscopy.

2. Principle of Acoustic Imaging

Figure 1 is the schematic diagram of the SAM. Referring to Fig. 1, the imaging principle of SAM is described as follows:

The SAM instrument comprises a transmitting/receiving section, an X-Y scanning section, a Z scanning section, a computer section for controlling the SAM, and a display section for observing a specimen. The transmitting/receiving section includes a transmitter, a receiver having an amplifier, and a circulator. The X-Y scanning section comprises an X-Y stage including a temperature-controlled chamber for containing living cells grown on a substrate in a coupling medium (*i.e.*, a culture liquid). The Z scanning section includes a Z-stage and an acoustic lens. An electrical signal (*i.e.*, tone-burst wave) generated by a transmitter inputs to a piezoelectric transducer (*i.e.*, zinc oxide), located on the top of a buffer rod through a circulator. The input voltage from the transmitter to the transducer is approximately 5V. The electrical signal is converted into an acoustic signal (*i.e.*, ultrasonic plane wave) by the transducer. The ultrasonic plane wave travels through the buffer rod made of sapphire to a spherical recess (hereinafter

*1 E-mail: miyasc@inel.gov, Telephone: 208-526-8951, Facsimile: 208-526-0690

*2 E-mail: a36@psu.edu, Telephone: 814-863-0152, Facsimile: 814-863-7024

called simply the “lens”) located at the bottom of the buffer rod, wherein the lens is coated by the acoustic impedance matching layer which is a so-called “acoustic anti-reflection coating” made of silicon oxide (hereinafter called simply “AARC”). The lens converts the ultrasonic plane wave to an ultrasonic spherical wave (*i.e.*, ultrasonic beam).

The ultrasonic beam is focused within the cells grown on the substrate located at the bottom of the chamber, and reflected from the cells via the culture liquid. The temperature of the culture liquid is constantly maintained at 37°C. The reflected ultrasonic beam, which carries acoustic information of the cells, is again converted into an ultrasonic plane wave by the lens. The ultrasonic plane wave returns to the transducer through the buffer rod. The ultrasonic plane wave is again converted into an electrical signal by the transducer. The voltage of the electric signal ranges from 300mV to 1V. When the operating frequencies range from 100MHz to 1GHz, the corresponding values for the insertion loss range from approximately 30dB to 80dB. Therefore, the electric signal must be amplified by 30dB to 80dB at a receiver.

Furthermore, the electric signal comprises transmission leaks, internal reflections from the interface between the lens and the AARC, and reflections from the specimen. Therefore, the reflections must be selected by a rectangular wave from a double balanced mixer (hereinafter called simply “DMB”) that is so-called the “first gate.” Then, the peak of the amplitude of the electric signal is detected by a circuit, which includes a diode and a capacitor (*i.e.*, the peak detection technique). The gate noise is removed by using the second gate existing within the first gate (*i.e.*, the blanking technique). The peak-detected signal is stored into a memory through an analog-to-digital signal (hereinafter called simply “A/D”) converter. The stored signal is again converted into an analog signal by a digital-to-analog signal (hereinafter called simply “D/A”) converter. This flow of processes allows the information that is collected at a single spot on the cells to be displayed as intensity at a certain point on the CRT monitor.

In order to form a two-dimensional acoustic image, an acoustic lens and an X-Y stage are mechanically scanned across a certain area of the cells. The scanned area determines the magnification of the image. The acoustic lens is able to translate axially along the z direction to vary the distance between the cells and the lens for sub-surface visualization. That is, when visualizing the bottom of the cells, the acoustic lens is focused on the substrate (we denote $z = 0\mu\text{m}$), and when visualizing a subsurface of the cells, the acoustic lens is mechanically defocused toward the lens (we denote $z = +x\mu\text{m}$, where x is the defocused distance).

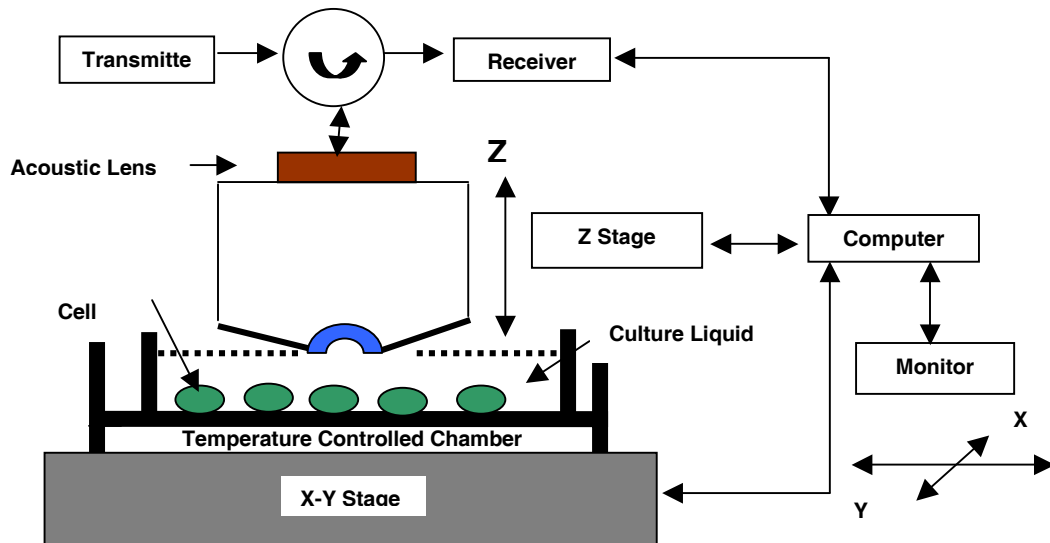


Fig. 1: Schematic diagram of SAM

3. Specimens

For the SAM experiments, MC3T3-E1 osteoblasts were plated at 10^4 cells/cm² in differentiation medium (MEM + 10% FBS, 50ug/ml ascorbic acid, and 10m, glycerophosphate) and incubated overnight. The following day, media were replaced with 50% 2x differentiation medium (MEM + 20% FBS, 100ug/ml ascorbic acid, and 20mM, glycerophosphate) plus 50% MDA-MB-231 conditioned medium or vehicle control medium (serum free medium). Cells were cultured in a humidified 37° incubator containing 5% CO₂ and 95% air, receiving media changes every other day. For the laser scanning confocal microscopy experiments, cells were fixed in 4% paraformaldehyde and stained with either AlexaFluor 568 phalloidin (twenty minutes) or monoclonal anti-tubulin cy-3 conjugate (one hour). Focal adhesion plaques can be visualized by interference reflection microscopy was used to visualize the focal adhesion as black spots [13]-[15]. However, it is unclear (see Fig. 2).

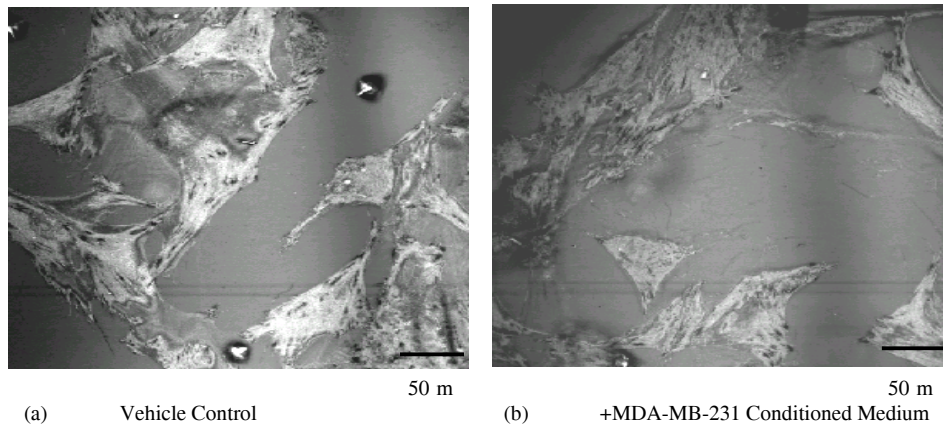


Figure 2: Focal adhesion plaques (black spots) were visualized using interference reflection microscopy.

4. Scanned Image Microscopy

4.1 LASER SCANNING CONFOCAL MICROSCOPY

Figure 3(a) is the laser scanning confocal microscope (hereinafter called simply “LSCM”) image of normally cultured osteoblasts, and Fig. 3(b) is the LSCM of osteoblasts cultured in cancer conditions. The cytoskeletons are highly resolved in Fig. 3. However, it is very difficult to judge whether delaminations exist at the interface between the cells and the substrate in Fig. 3(b). Figure 3(c) is a vertical cross-sectional image for measuring the thickness of the cell. The average thickness of osteoblasts is typically 10µm. Based on these images, we can select an appropriate frequency to observe the condition of the interface between the cell and the substrate with SAM.

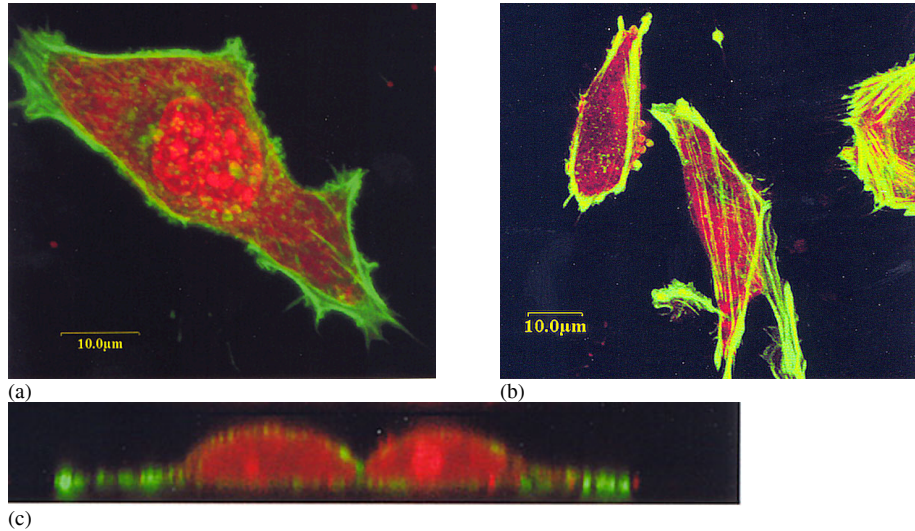


Figure 3: LSCM images of MC3T3-E1 osteoblasts. (a) MC3T3-E1 osteoblasts cultured with 50% vehicle control medium, (b) MC3T3-E1 osteoblasts cultured with 50% MDA-MB-231 conditioned medium for two days. Note the patterned cobblestone appearance of the vehicle control cells compared to the long, spindle-like morphology of cells cultured with the cancer-conditioned medium (c) Thickness measurement with LSCM

4.2 SCANNING ACOUSTIC MICROSCOPY

4.2.1 Resolution and Contrast

It is better to use an ultrasonic frequency at 1.0GHz or more to observe highly resolved details of biological cells with SAM. In high frequency medical acoustic imaging, contrast is an important factor as well as the resolution. Figures 4(a), 5(a) show the surface of the resolution chart with the conventional optical microscope, and with the SAM with a frequency at 1.0GHz. Figure 5(a) is a specimen having patterns for measuring a lateral resolution of the surface for the SAM. Figure 4(b) is a vertical cross-sectional view of a specimen for measuring subsurface resolution. From the acoustic image, the surface resolution with frequency at 1.0GHz is 0.7 μm, but the subsurface resolution cannot be measured (see Fig. 5(b), where “*d*” is set at 10 μm). It means that a high frequency such as 1.0GHz or more may not be used for this study.

The cells have acoustic impedances close to those of the culture liquid and virtually no contrast caused by the difference in reflection coefficient can be displayed. However, the contrast in the acoustic images can be generated from the difference in attenuation. When using a background (*i.e.*, substrate) composed of highly reflective materials such as sapphire with an acoustic impedance of $44.3\text{kg/m}^2 \times 10^6$, the difference in attenuation of the cells can be maximized in the image. This method is useful, when operating SAM at a frequency of 1.0GHz or more. However, osteoblasts are relatively thick (thickness range: 7~13 μm), so that attenuation is too high to visualize the interface between the cells and the sapphire substrate with higher ultrasonic frequency such as 1.0GHz in the culture liquid at the temperature of 37°C. The frequency to visualize them is limited to approximately 600MHz in this study.

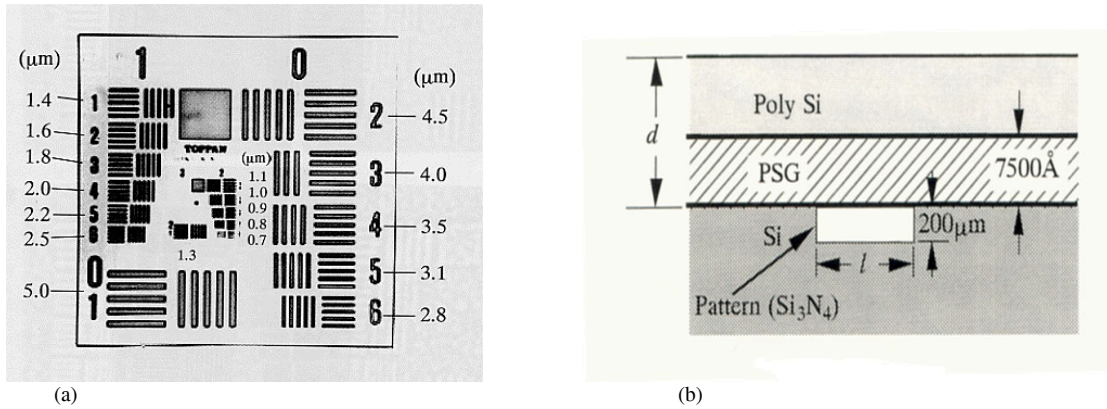


Figure 4: (a) Resolution Chart (Optical Image) to measure subsurface resolution, (b) A vertical cross-sectional view of a resolution chart to measure subsurface resolution, wherein “ d ” is the thickness of the coating indicating the penetration depth of SAM, and “ l ” is the internal lateral resolution of the SAM.

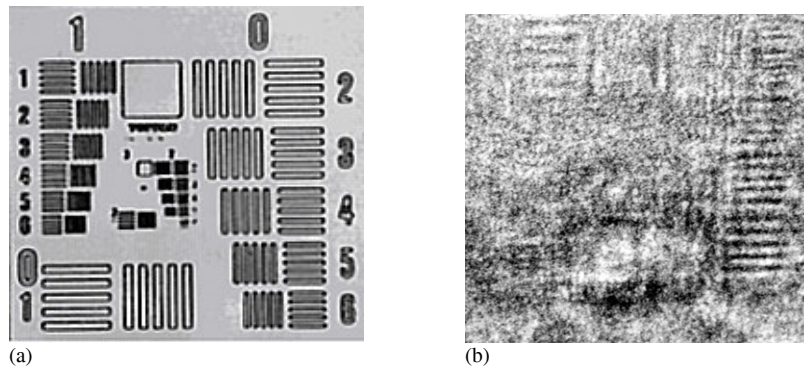


Figure 5: Acoustic images with frequency at 1.0GHz, (a) the surface resolution chart, (b) the subsurface resolution with $d = 100\text{m}$.

4.2.2 Acoustic Imaging of Cells

An acoustic beam (*i.e.*, spherical longitudinal wave) emitted from the lens via the culture liquid is focused onto the substrate in Fig. 5 (a). The acoustic impedance of gas, such as air, is significantly lower than that of the cell. Therefore, theoretically, if the interface between the cell and the substrate has an adhesive problem (*e.g.*, a delamination), the acoustic wave will reflect strongly from the interface. The contact area having the adhesive problem is observed as a high intensity (white) region in the acoustic image. In Fig. 6(a), we can unclearly observe such areas. We can think of at least two reasons for this phenomenon; first, the acoustic impedance of the cell is close to the culture liquid; second, the gap may be too thin comparing to the wavelength of the longitudinal ultrasonic beam. Since the aperture angle of the lens is large (*i.e.*, 120°), we propose that we defocus the acoustic lens toward the substrate to generate a surface acoustic wave (SAW) when observing the adhesive problem at the interface. The wavelength of the SAW is substantially less than half of that of the longitudinal wave. Furthermore, the SAW is very sensitive to discontinuities. Therefore, we have an opportunity to see the adhesive problem at the interface. Figures 6(b), 6(c) and 6(d) show the adhesive problem (*i.e.*, “white” areas) at the interface that the conventional optical microscopy cannot visualize. In addition, we see some internal details of the cells. In addition, we observed fixed osteoblasts with SAM (see Fig. 7). As can be appreciated, the shapes of the cells are totally different from those of the living cells in Figs. 6(a) and 6(b). Our assumption is that the fixing procedure for the cells, when we try to observe the adhesive conditions with optical microscopy, may have an effect on the interface.

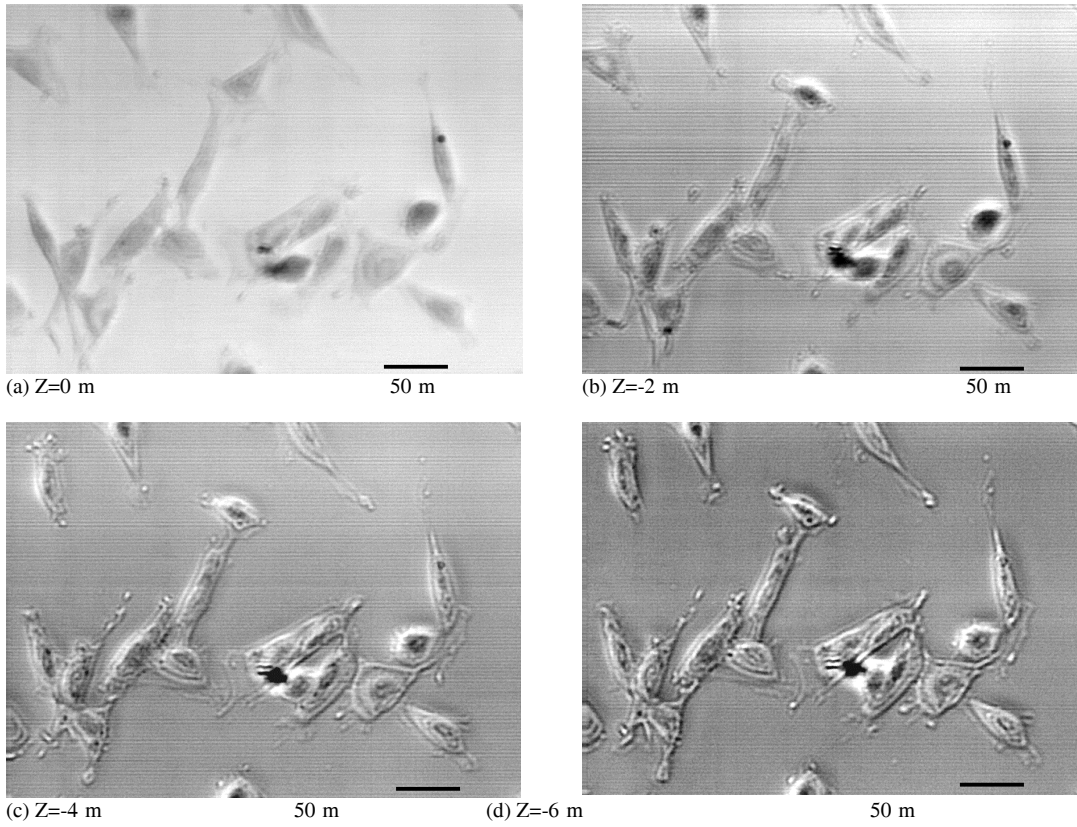


Figure 6: SAM images of MC3T3-E1 osteoblasts cultured with 50% MDA-MB-231 conditioned medium for 2days.

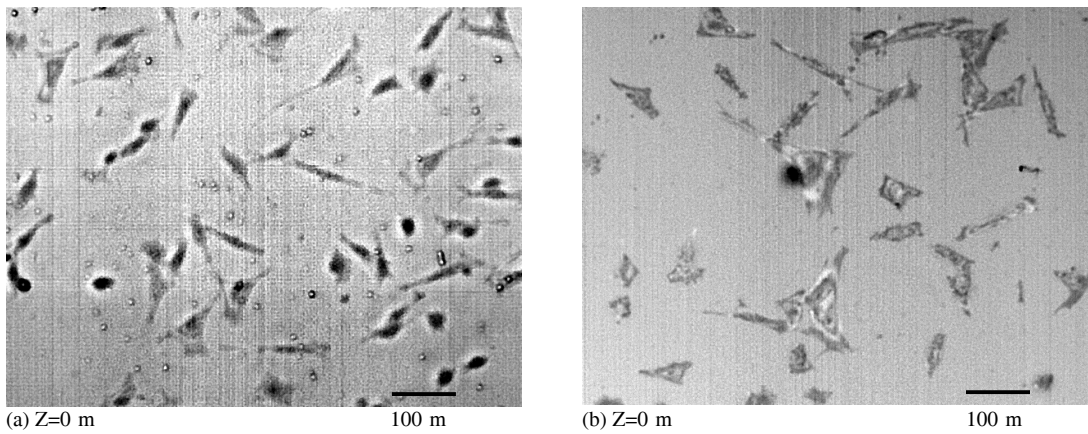


Figure 7: SAM (frequency: 400MHz) images of fixed MC3T3-E1 osteoblasts cultured with 50% MDA-MB-231 conditioned medium for 2days. The cells were cultured on the plastic substrate, (a) 1% glutaraldehyde (b) 4% glutaraldehyde

6. Conclusion

There are at least two important results in this study. One is that the SAM has the advantage of allowing surface and subsurface imaging of biological living cells. Comparison with images obtained with the LSCM show astonishing differences because the staining and fixing process appears to dramatically deform the cells. Another is that the defocusing of the acoustic lens toward to the substrate brings out many important features in the cell imaging. This is seen in part as a result of constructive interference between longitudinal and leaky surface waves which agrees with well known the $V(z)$ curve theory [16]-[18].

7. Acknowledgement

Robin. R. Mercer was supported by a pre-doctoral grant from the US Army Medical Research Materiel Command under DAMD 17-02-1-0358. Research was supported in part by a Biotechnology Grant, Life Sciences Consortium, the Pennsylvania State University, PA Tobacco Settlement Fund, the National Foundation for Cancer Research, Center for Metastasis Research, the USMC Research university that resides at the Pennsylvania State University under Contract M67004-99-0-0037, U.S. Department of Energy, Office Basic Energy Sciences, Materials and Engineering Physics under DOE Idaho Operations Office Contract DE-AC07-99ID13727.

8. References

1. Landis, S. H., Murray, T., Bolden, S., Wingo, P. A. (1999), Cancer statistics, *CA Cancer J. Clin* **49(1)**, 31, 8-31.
2. Galasko, C. S., (1982) Mechanisms of lytic and blastic metastatic disease of bone, *Clin Orthop* (169), .20-27.
3. Delmas, P. D., Demiaux, B., Malaval, L., Chapuy, M. C., Edouard, C., Meunier, P. J. (1986): Serum bone gamma carboxyglutamic acid-containing protein in primary hyperparathyroidism and in malignant hypercalcemia. Comparison with bone histomorphometry, *J. Clin Invest* **77(3)**, 985-991. .
4. Stewart, A. F, Vignery, A., Silverglate, A., Ravin, N. D., LiVolsi, V., Broadus, A. E., Baron, R. (1982): Quantitative bone histomorphometry in humoral hypercalcemia of malignancy: uncoupling of bone cell activity, *J. ClinEndocrinol Metab* **55(2)**, 219-227.
5. Taube, T., Elomaa, I., Blomqvist, C., Beneton, M. N., Kanis, J. A. (1994): Histomorphometric evidence for osteoclast-mediated bone resorption in metastatic breast cancer, *Bone* **15(2)** 161-166.
6. Atalar, A., Quate, C. F., and Wickramasinge, H. K. (1977): "Phase imaging in reflection with acoustic microscope, *Appl. Phys. Lett.*, **31**, 791-793.
7. Hildebrand, J. A., Rugar, D., Johnston, R. N., and Quate, C. F. (1981): Acoustic microscopy of living cells," *Proc. National Academy of Science*, **78(3)**, 1656-1660.
8. Hildebrand, J. A. (1985): Observation of Cell-Substrate Attachment with the Acoustic Microscope, *IEEE Transaction on Sonic and Ultrasonics*, **SU-32**, No. 2, 332-340.
9. Bereiter-Hahn, J. (1986): Scanning acoustic microscopy visualizes cytomechanical responses to cytochalasin D, *J. Microsc.* **146**, 29-39.
10. Bereiter-Hahn, J. and Lüers, H (1990): Shape changes and force distribution in locomoting cells. Investigation with reflected light and acoustic microscopy, *Eur. J. Cell Biol.* **53**: Suppl. 31, .85-91.
11. Tittmann, B. R. and Miyasaka, C. (2003): Imaging and Quantitative Data Acquisition of Biological Cells and Soft Tissues with Scanning Acoustic Microscopy, In *Science, Technology and Education of Microscopy: An Overview*. Fomatex: Badajoz, Spain, 325-344.
12. Tittmann, B. R. and Miyasaka C., (2002): Thermal and Acoustical Insult to Cells as Studied by In-Vivo Acoustic Microscopy," Presented at the 2002 ASME Pressure Vessels and Piping Conference, Aug. 4-8, Vancouver, British Columbia. *NDE Engineering: Applications* edited by G. Ramirez, C. Miyasaka, and O. Hedden, PVP-Vol. 450, NDE-Vol. 22, The American Society of Mechanical Engineers, New York, NY, 43-48.
13. Gingel, D. and Todd, I. (1979): Interference Reflection Microscopy: A Quantitative Theory for Image Interpretation and its Application to Cell-Substrate Separation Measurement, *Biophys. J.*, **26**, 507-526.
14. Bereiter-Hahn, J., Fox, C. H., and Thorell, B. (1979): Quantitative Reflection Contrast Microscopy of Living Cells, *J. Cell Biol.* **82**, 767-779.
15. Mercer R., Miyasaka C., and Mastro, A. M. Metastatic Brest Cancer Cells Suppress Osteoblast Adhesion and Differentiation," *Clinical and Experimental Metastasis*. (in Press)
16. Weglein R. D. (1979): A model for predicting acoustic materials signatures", *Appl. Phys. Lett.*, **34**, 179-181
17. Parmon W., and Bertoni, H. L. (1979): Ray interpretation of the material signature in the acoustic microscope, *Electron. Lett.*, **15**, 684-686
18. Atalar , A. (1978): An angular spectrum approach to contrast in reflection acoustic microscopy, *J. Appl. Phys.*, **49**, 5130-5139,